Electronic Supplementary Material (ESI) for New Journal of Chemistry.

Electronic Supplementary Information

Synthesis and Characterization of Low Viscosity Hexafluoroacetylacetonate-based Hydrophobic Magnetic Ionic Liquids

Stephen A. Pierson[a], Omprakash Nacham[a], Kevin D. Clark[a], He Nan[a], Yaroslav Mudryk[b], and Jared L. Anderson[a]*

[a]*Department of Chemistry, Iowa State University, 1605 Gilman Hall, Ames, IA 50011, USA.*

[b]*Division of Materials Science and Engineering, Ames Laboratory, Iowa State University, 254 Spedding, Ames, IA 50011, USA*

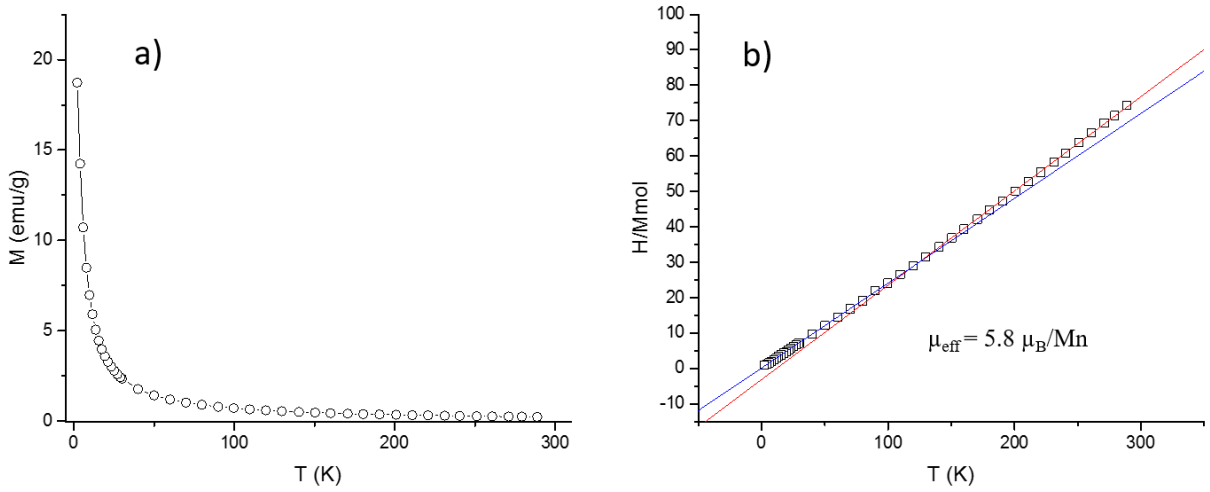

Figure S1. (a) Magnetization of the $[P_{66614}^{+}][Mn(II)(hfacac)_3^{-}]$ MIL measured as a function of temperature in a 20000 Oe applied magnetic field (b) Curie-Weiss fits of both high- and low-temperature linear regions of the reciprocal susceptibility

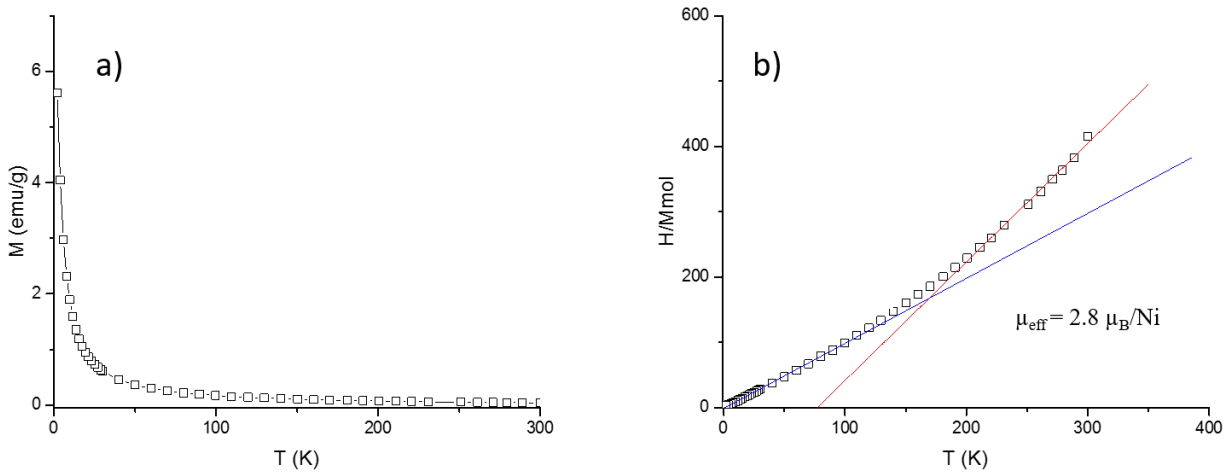

Figure S2. (a) Magnetization of the $[P_{66614}^{+}][Ni(II)(hfacac)_3^{-}]$ MIL measured as a function of temperature in a 20000 Oe applied magnetic field (b) Curie-Weiss fits of the linear regions of the reciprocal susceptibility above and below the ~150 K anomaly.

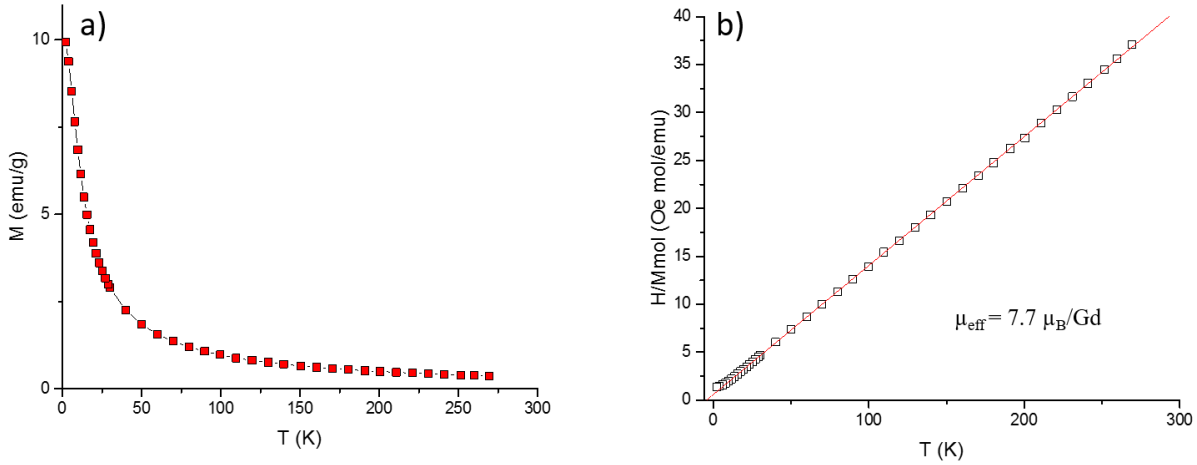

Figure S3. (a) Magnetization of the $[P_{66614}^{+}][Gd(III)(hfacac)_4^{-}]$ MIL measured as a function of temperature in a 20000 Oe applied magnetic field (b) Curie-Weiss fit of the linear portion of the reciprocal susceptibility.

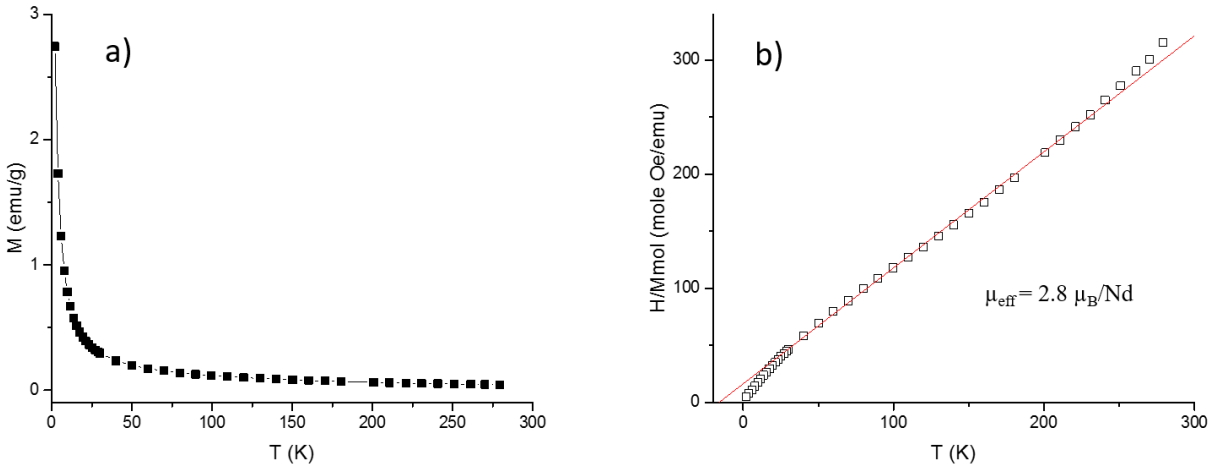

Figure S4. (a) Magnetization of the $[P_{66614}^{+}][Nd(III)(hfacac)_4^{-}]$ MIL measured as a function of temperature in a 20000 Oe applied magnetic field (b) Curie-Weiss fit of the linear portion of the reciprocal susceptibility.

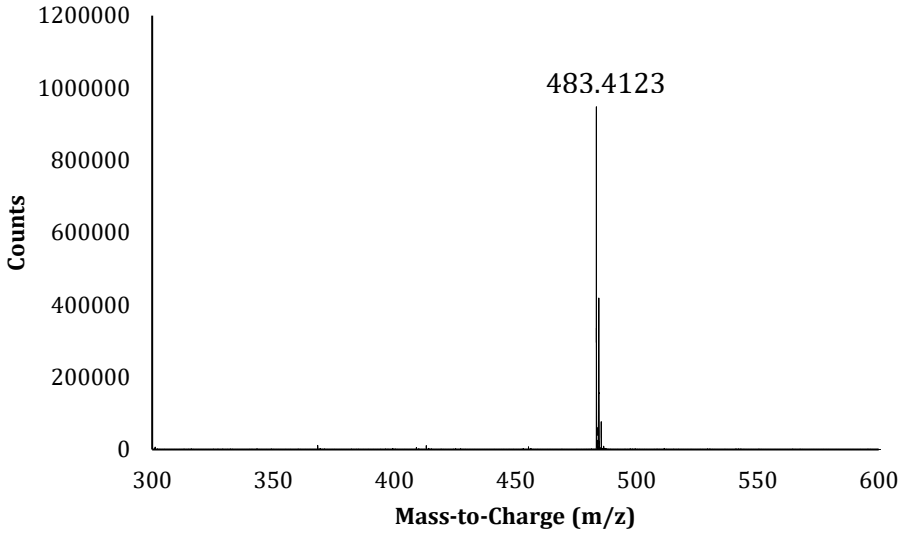

Figure S5. Mass spectrum of $[P_{66614}^{+}]$ using TOF LC/MS (positive mode).

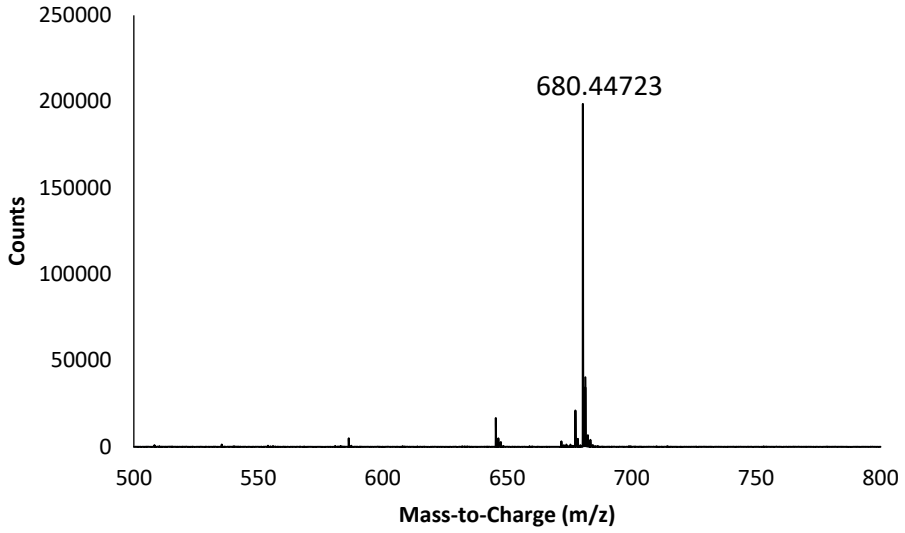

Figure S6. Mass spectrum of [Co(II)(hfacac)$_3^-$] using TOF LC/MS (negative mode).

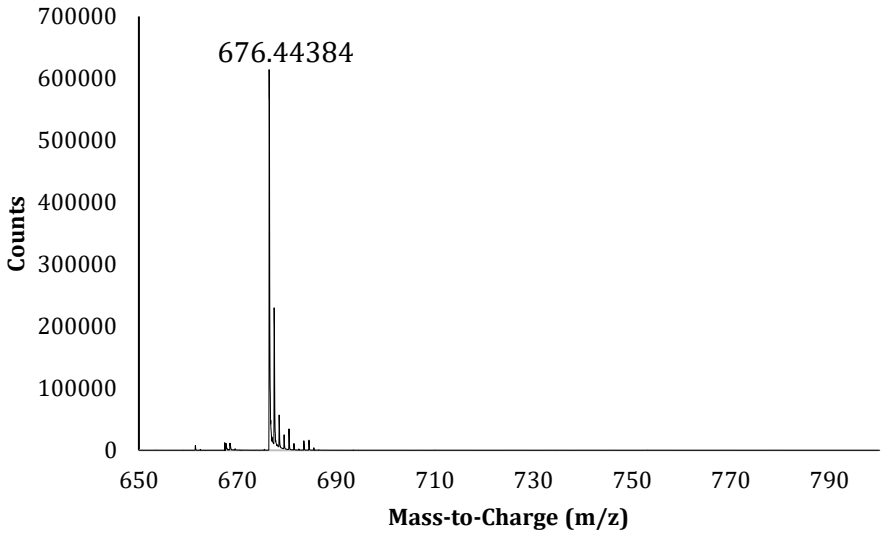

Figure S7. Mass spectrum of [Mn(II)(hfacac)$_3^-$] using TOF LC/MS (negative mode).

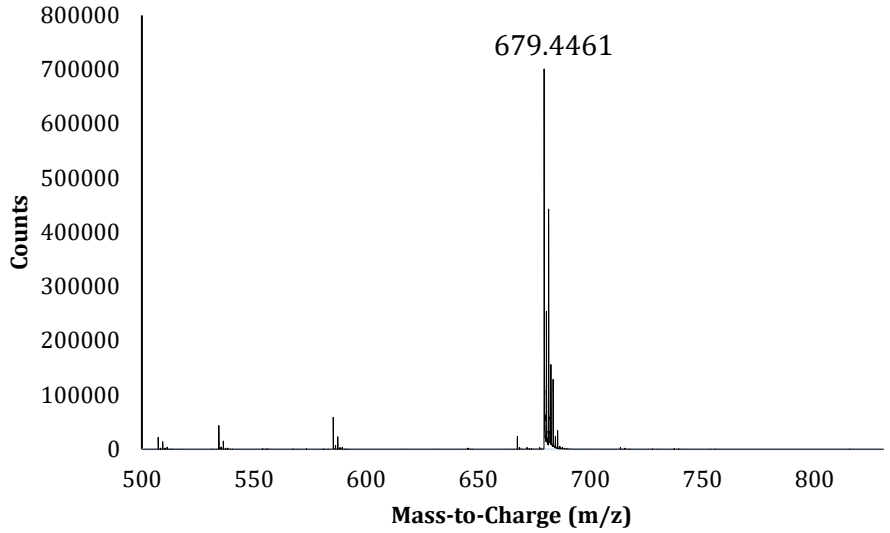

Figure S8. Mass spectrum of [Ni(II)(hfacac)$_3^-$] using TOF LC/MS (negative mode).

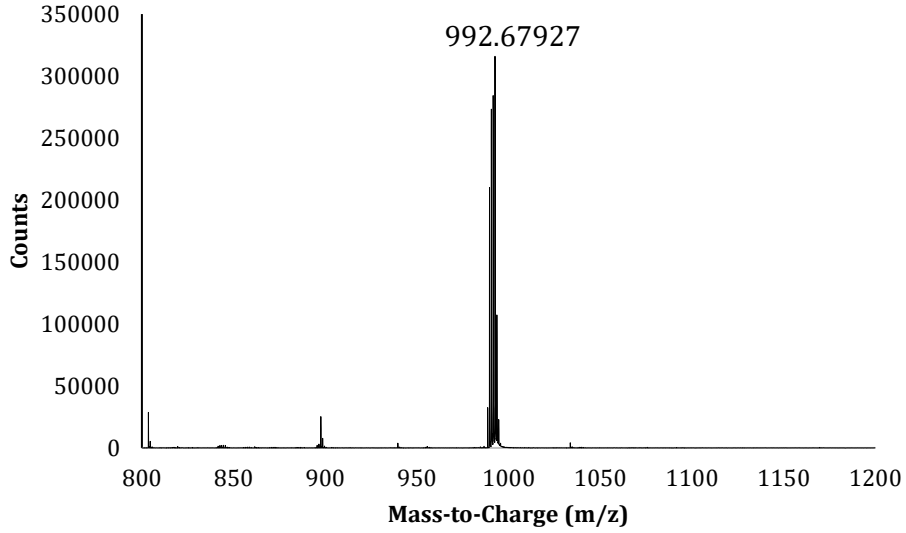

Figure S9. Mass spectrum of [Dy(III)(hfacac)$_4^-$] using TOF LC/MS (negative mode).

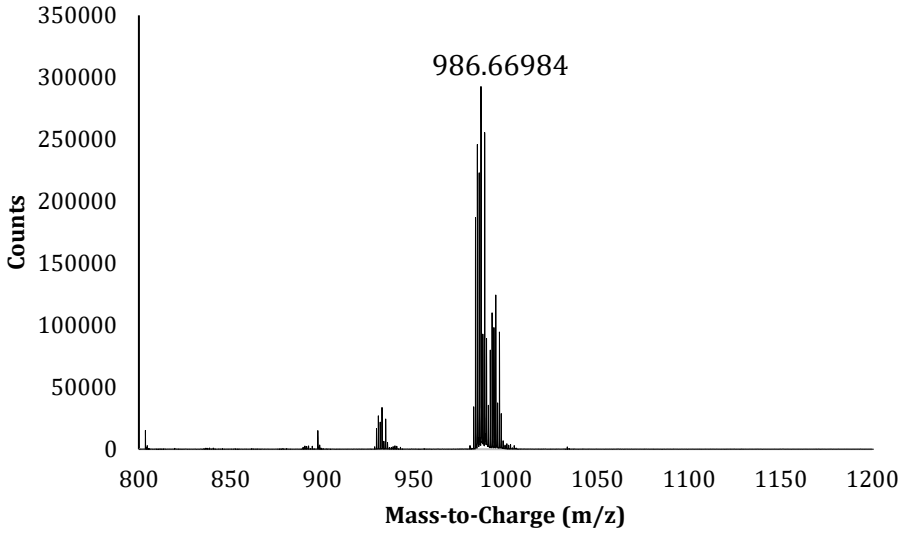

Figure S10. Mass spectrum of [Gd(III)(hfacac)$_4^-$] using TOF LC/MS (negative mode).

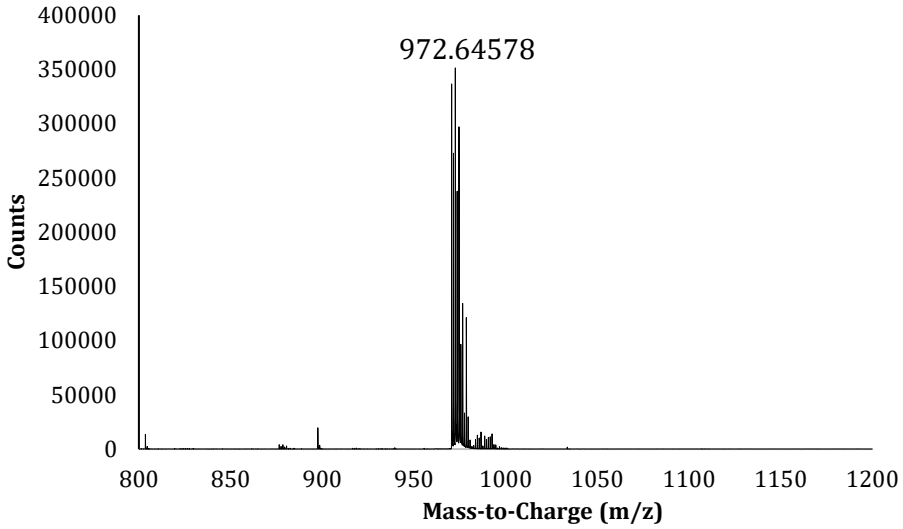

Figure S11. Mass spectrum of [Nd(III)(hfacac)$_4^-$] using TOF LC/MS (negative mode).

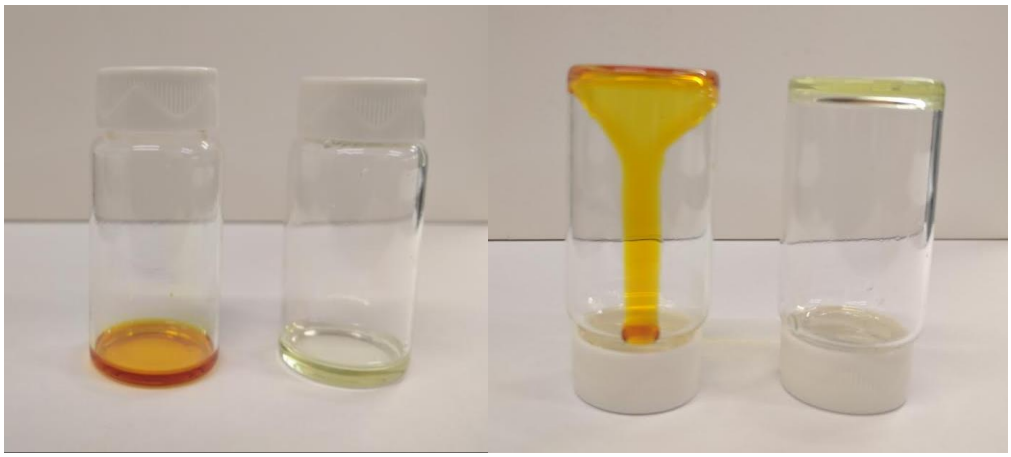

Figure S12. $[P_{66614}^{+}][Mn(II)(hfacac)_3^{-}]$ (left) and $[P_{66614}^{+}]_2[MnCl_4^{2-}]$ (right) before and after inversion for 2 seconds.

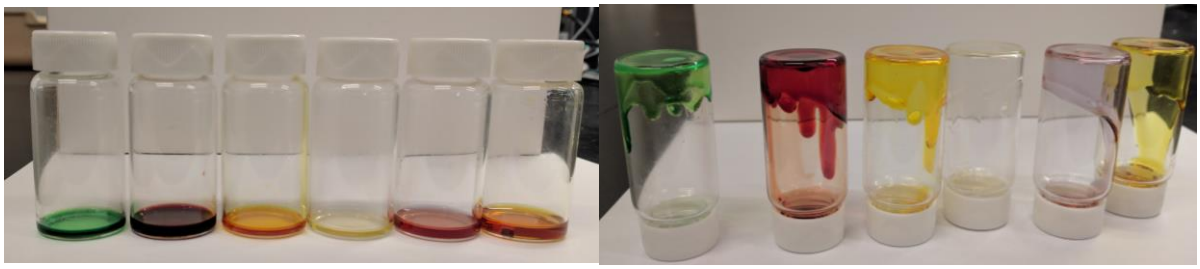

Figure S13. From left to right: $[P_{66614}^{+}][Ni(II)(hfacac)_3^{-}]$, $[P_{66614}^{+}][Co(II)(hfacac)_3^{-}]$, $[P_{66614}^{+}][Mn(II)(hfacac)_3^{-}]$, $[P_{66614}^{+}][Dy(III)(hfacac)_4^{-}]$, $[P_{66614}^{+}][Nd(III)(hfacac)_4^{-}]$, and $[P_{66614}^{+}][Gd(III)(hfacac)_4^{-}]$ before and after inversion for 1 second.